Chemoproteomics Unveils the Antibacterial Mechanism of Silver Ions: Inhibiting Peptidoglycan Synthesis via Targeting Mur Family Proteins in *Staphylococcus aureus*

Lirun Zhou[a,b,#], Ying Zhang[b,c,#], Yajian Li[d], Tong Yang[b], Zheng Chu[b], Qianyu Zhang[b], Hechen Tang[b], Ang Ma[b], Peng Gao[b], Chen Wang[b], Yin Kwan Wong[e], Cui Liu[b], Shengnan Shen[b], Junzhe Zhang[b], Qiaoli Shi[b], Huan Tang[b,*], and Jigang Wang[a,b,c,*]

Supporting Information

Experimental Section

Figure S1. Biosynthesis of peptidoglycan in *S. aureus*. This figure illustrates the biosynthetic pathway of peptidoglycan in *S. aureus*, highlighting the key enzymes involved in its synthesis. The process begins with the formation of UDP-MurNAc-pentapeptide, which serves as the precursor for peptidoglycan. The enzymes MurA to MurF catalyze the sequential steps in the cytoplasm, leading to the generation of the lipid-linked intermediates. These intermediates are subsequently transported across the cytoplasmic membrane, where further modifications and polymerization occur to form the peptidoglycan structure. The final peptidoglycan layer plays a critical role in maintaining the structural integrity of the bacterial cell wall.

Figure S2. Bacterial survival rate of *S. aureus* following 24 hours of treatment with amoxicillin at various concentrations (n = 6).

Figure S3. Bacterial survival rate of *Escherichia coli* following 24 h of treatment with Ag^+ at different concentrations (n = 6).

Figure S4. 50% inhibitory concentrations (IC_{50}) of Ag^+ on the enzymatic activity of WT murC protein.

Figure S5. (A) Protein-based thermal shift assays showing the thermal stability of MurB in the absence and presence of Na^+ (1 μM). (B) Protein-based thermal shift assays showing the thermal stability of MurC in the absence and presence of Na^+ (1 μM). (C) Protein-based thermal shift assays showing the thermal stability of MurD in the absence and presence of Na^+ (1 μM).

Figure S6. (A) The binding affinity of MurB to Na^+, measured by microscale thermophoresis. (B) The binding affinity of MurC to Na^+, measured by microscale thermophoresis. (C) The binding affinity of MurD to Na^+, measured by microscale thermophoresis.

Figure S7. Bactericidal activity of Ag^+ against *Staphylococcus aureus* at concentrations used in the biofilm assays(n=6).

Reference

Materials and methods

Reagents

Tris(2-carboxyethyl)phosphine hydrochloride (TECP), TAMRA-azide, Biotin-azide, Tris[(1-benzyl-1H-1,2,3-triazol-4-yl)methyl]amine (TBTA), Biotin-alkynyl, Copper (II) sulfate ($CuSO_4$), and TAMRA-alkynyl were obtained from Sigma-Aldrich (USA). The Pierce™ Quantitative Fluorometric Peptide Assay Kit, NeutrAvidin agarose beads, dimethyl reagent, sequencing-grade modified trypsin, and tetraethylammonium bromide (TEAB) were purchased from Thermo Fisher Scientific (USA).

Cell and *S. aureus* culture

RAW 264.7 (RRID: CVCL_0493) and BEAS-2B (RRID: CVCL_0168) cells were obtained from the Chinese Academy of Medical Sciences (Beijing, China). Cells were cultured in DMEM (Corning, USA) supplemented with 10% FBS (Corning, USA) and 100 IU/mL penicillin–streptomycin (Thermo Fisher, USA), and maintained at 37 ℃ in a humidified incubator with 5% CO_2.

Staphylococcus aureus (ATCC 6538) was obtained from Shanghai Luwei Technology Co., Ltd. and stored at -80 ℃. For activation, a 100 μL aliquot of the bacterial suspension was evenly spread on LB agar plates (containing 1 g NaCl, 0.5 g yeast extract, 1 g tryptone, and 1.5 g agar per 100 mL) and incubated at 37 ℃ for 24 hours. Smooth colonies were then inoculated into 30 mL of LB broth and cultured in a shaker incubator at 37 ℃ and 120 rpm for 18 hours. Bacteria in the stationary growth phase (OD_{600} = 1.0) were harvested for subsequent experiments.

Cell viability

RAW 264.7 and BEAS-2B cells were seeded in 96-well plates at a density of 1.0 × 10^4 cells per well and allowed to adhere for 24 h. The cells were then treated with varying concentrations of Ag^+ for a further 24 h. Cell viability was subsequently determined using a CCK-8 Kit (Dojindo, Japan) in accordance with the manufacturer's

protocol. Absorbance was measured at 450 nm using a multimode plate reader (PerkinElmer, USA).

MIC determination of Ag^+ and amoxicillin

Ag^+ (16 μM) and amoxicillin (100 nM) were subjected to serial twofold dilutions (1:2–1:256) in LB broth. Aliquots (100 μL) of each dilution were dispensed into 96-well plates, followed by the addition of 10 μL of *S. aureus*, MRSA, or *E. coli* suspensions (5×10^5 CFU per well). Plates were incubated for 24 h. Bacterial growth was then assessed by measuring optical density at 600 nm, and the minimum inhibitory concentrations (MICs) were determined accordingly.

Plate colony counting method

Ag^+ was diluted in LB liquid medium to predetermined concentrations, and each medium was inoculated with 10 μL of *S. aureus* at a concentration of 5×10^5 CFU. After an initial incubation at 37 ℃ for 6 h, the samples were further diluted 1:1000, and 100 μL of the diluted solution was plated onto LB solid media. The plates were further incubated at 37 ℃ for 24 h, after which colony counts were determined.

Checkerboard Assay

After mixing Ag^+ and amoxicillin at their 2×MIC concentrations, a gradient dilution was performed to determine the MIC after mixing. The FIC is calculated as follows: FIC = (MIC of Ag^+ in combination / MIC of Ag^+ alone) + (MIC of Amoxicillin in combination / MIC of Amoxicillin alone). FIC ≤ 0.5 demonstrates synergy, 0.5 < FIC < 2 indicates no difference, and FIC ≥ 2 indicates antagonism between the two agents.

Growth curve and killing curve

Bacterial suspensions of *S. aureus* were prepared in LB broth, with OD_{600} values adjusted to 0.2 for the growth curve and 0.6 for the killing curve experiments. The suspensions were incubated with various concentrations of Ag^+ at 37 ℃ under

continuous shaking at 160 rpm. At designated time intervals, the optical density at 600 nm (OD_{600}) of 1-mL samples was measured using a micro-spectrophotometer (1).

Competitive in-gel fluorescence labeling assay

For *in situ* fluorescence labeling, activated *S. aureus* was grown in 150 mL LB broth at 37 ℃ for 18 h (OD_{600} = 1.0). Cells were collected by centrifugation at 8000 rpm for 10 min and resuspended in 1 mL LB medium. Ag^+ was then added, followed by an additional 8 h incubation. The bacterial cells were subsequently washed three times with PBS.

After protein quantification, samples were labeled with the cysteine-reactive probe IAA-yne at 37 ℃ for 1 h with shaking. A click reaction mixture (13 μL total) was then added to each sample, consisting of TBTA (9 μL, 10 mM in DMSO), TCEP (3 μL, 50 mM in ddH_2O), $CuSO_4$ (3 μL, 50 mM in ddH_2O), and TAMRA-azide (1 μL, 10 mM in DMSO). The reaction was allowed to proceed for 2 h at 37 ℃ with agitation.

Proteins were precipitated by adding 1 mL acetone and incubating at −20 ℃ for 12 h, followed by centrifugation at 20,000 g for 10 min. The supernatant was removed, and the protein pellet was resuspended in 100 μL of 1× loading buffer. Samples were denatured at 90 ℃ for 5 min prior to separation by 12% SDS–PAGE. Fluorescent signals were detected using an Azure Sapphire RGB NIR scanner (USA), and total protein loading was confirmed by Coomassie Brilliant Blue (CBB) staining.

Streamlined cysteine activity-based protein profiling

To identify potential protein targets of Ag^+ in *S. aureus*, we performed competitive mass spectrometry experiments using a novel DBIA probe (ChomiX Biotech Co., Nanjing, China). Three experimental groups were established: 200 μM DBIA, 100 μM Ag^+ + 200 μM DBIA. The probe labeling process was like the in-gel fluorescent labeling of Ag^+ in *S. aureus* described above. First, 200 μM DBIA was added to 100 μL of Ag^+-treated cell lysis and incubated for 1 hour. Next, 5 mM DTT and 20 mM IAA were added to alkylate the reduced cysteine residues, and the reaction was allowed

to proceed for 30 minutes in the dark. Following alkylation, 2 μg of trypsin and Lys-C (Thermo Scientific, USA) were added to digest the protein. For the peptide labeling process, all TMTs were labeled with DBIA-containing cysteines conjugated according to the dimethyl Mass Tag reagent (Thermo Scientific, USA). For peptide enrichment, 100 μL of beads (Thermo Scientific, USA) were added to the dimethyl-labeled mixed sample dissolved in 1 mL of PBS. To remove nonspecific binding, the beads were washed three times with 1 mL PBS, 1 mL 0.1% SDS, and 1 mL ddH_2O. Finally, the enriched peptides were analyzed using an Orbitrap Fusion Lumos mass spectrometer (Thermo, USA) via LC-MS/MS.

Whole-proteome experiment

S. aureus was seeded into 15-mL centrifuge tubes and treated with 0.5 μM Ag^+ or ddH_2O for 12 h before cell lysis was collected. The protein concentration was determined using a BCA assay. Next, 5 mM DTT and 10 mM IAA were added for 30 min to alkylate cysteine residues. The samples were then digested overnight with trypsin at 37 ℃ and desalted using a commercial C18 column prior to further analysis.

Expression and purification of MurB, MurC, MurD, MurB(C224A), MurC(C368A), and MurD(C221A) protein

Recombinant MurB, MurC, MurD, and their mutant variants (MurB(C224A), MurC(C368A), MurD(C221A)) were subcloned into the pET29A, pET29B, and pET-15b vectors, respectively, with a 6 × His-tag fusion (Sheng gong, Shanghai, China). The recombinant plasmids were introduced into *E. coli* BL21 cells and cultured in LB medium supplemented with kanamycin (50 μg/mL) at 37 ℃ with shaking until the OD_{600} = 1.0. Protein expression was then induced with 0.4 mM IPTG, followed by incubation at 17 ℃ for 14 h. Cells were harvested by centrifugation, resuspended in lysis buffer (200 mM NaCl, 20 mM Tris-HCl, 1 mM PMSF, pH 8.0), and lysed by sonication to obtain the target proteins. The precipitate was dissolved in inclusion body lysis buffer (Baiaolaibo, KD0688) and further extracted. The protein was then refolded using a refolding buffer (Baiaolaibo, KD0688). The samples were washed with PBS

and concentrated using a centrifugal filtration tube. Protein concentrations were determined by BCA assay, and the purity and integrity of the purified proteins were verified by SDS-PAGE gel electrophoresis.

Protein competition labeling of MurB, MurC, and MurD by IAA-yne

Five experimental groups were established for the competition labeling assay: a blank control group, an IAA-yne group, an Ag^+ competition group (with 5× and 10× concentrations), and an IAA competition group. Each group contained 5 μg of pure MurB, MurC, or MurD protein. The corresponding concentrations of Ag^+ or IAA were added to the Ag^+ competition and IAA competition groups, respectively, samples were then incubated at 37 ℃ with agitation at 800 rpm for 2 h. Next, 10 μM of IAA-yne was added to all groups except the control group, and incubation continued for an additional 1 h. A CLICK reaction was performed for 1 h, and upon completion, the proteins were denatured and analyzed by SDS-PAGE. Fluorescence was observed, and the samples were stained with CBB.

Protein-based Thermal Shift Assay

To investigate the interaction between Ag^+ and MurB, MurC, and MurD proteins, a Protein-based Thermal Shift Assay was employed. Briefly, pure MurB, MurC, and MurD protein samples were divided into two equal portions. One portion was incubated with Ag^+(1 μM), and the other with ddH_2O, at 37 ℃ for 1 hour. The mixtures were then transferred to tubes and exposed to defined temperatures (37, 42, 47, 52, 57, 62, and 67 ℃) for 3 minutes using a thermal cycler (Applied Biosystems, USA). After centrifugation, the supernatants were analyzed by SDS-PAGE, and the proteins were stained with CBB to assess binding.

Microscale thermophoresis (MST)

MST was employed to quantitatively assess the interaction between MurB, MurC, MurD, MurB(C224A), MurC(C368A), MurD(C221A), and Ag^+. The binding affinity was measured using a Monolith NT.115. Briefly, recombinant *S. aureus* MurB, MurC,

MurD, MurB(C224A), MurC(C368A), and MurD(C221A) proteins were labeled with fluorescence using the Monolith His-Tag Labeling Kit (Nano Temper Technologies, Munich, Germany). Ag^+ was serially diluted and mixed with the protein solution (50% v/v). The mixtures were loaded into capillaries and analyzed using MST at 40% power. The data were processed using MO Affinity Analysis software v2.3.

Molecular docking of Ag^+ with MurB, MurC and MurD

The structure of Ag^+ was obtained from PubChem, and the 3D structures of MurB, MurC, and MurD were retrieved from the AlphaFold Protein Structure Database. Both the protein and chemical structures were prepared by hydrogenation and dehydration using Autodock software (version 4.2.6), followed by molecular docking. Discovery Studio 2019 (version 2.5) and PyMOL software (version 2.5) were used to analyze and visualize intermolecular interactions.

MurC and MurC(C368A) enzyme activity assay

The inhibitory effect of Ag^+ on the MurC-catalyzed ligation of L-Ala to UDP-MurNAc in *S. aureus*, as well as on the MurC(C368A) mutant, was evaluated (2). Enzymatic activity was assessed by quantifying released phosphate using a modified malachite green colorimetric assay, as previously reported (3,4).

Briefly, reactions (50 μL total volume) were carried out in 50 mM HEPES buffer (pH 8.0) containing 3.25 mM $MgCl_2$, 120 μM UDP-MurNAc, 120 μM L-Ala, 450 μM ATP, and purified MurC or MurC(C368A) (prepared in 20 mM HEPES, pH 7.2, with 1 mM DTT). Test compounds, dissolved in DMSO, were added to a final concentration of 100 μM, with the DMSO content kept at 5% (v/v). For poorly soluble compounds, lower concentrations were used.

Following incubation at 37 ℃ for 15 min, reactions were terminated by adding 100 μL of Biomol reagent. After 5 min, absorbance was recorded at 650 nm, and enzyme activity was calculated based on the amount of phosphate released (3-5).

Dead/Live fluorescence staining assay

S. aureus was adjusted to an OD_{600} of 0.6. A bacterial control group and three experimental groups, each containing 5 mL of bacterial suspension, were established. The corresponding concentrations of Ag^+ were added to each treatment group, while the control group received an appropriate volume of ddH_2O. The samples were incubated at 37 ℃ with continuous agitation at 120 rpm for 10 h. Following incubation, live/dead cell was assessed using a Calcein-AM/PI staining kit (Solarbio, CAT: CA1630) in accordance with the manufacturer's protocol. Fluorescent images were captured using a confocal microscope.

Morphology observation of bacterial by SEM and TEM

S. aureus was adjusted to an OD_{600} of 0.6. A bacterial control group and three experimental groups, each containing 5 mL of bacterial suspension, were prepared. The corresponding concentrations of Ag^+ were added to each treatment group, while the control group received ddH_2O (37 ℃, 120 rpm for 10 h).

For TEM analysis, a 10 μL aliquot was placed onto a glow-discharged copper grid. The samples were stained with 0.4% uranyl acetate for 20 seconds before imaging (6).

For SEM analysis, the samples fixed overnight with 2.5% glutaraldehyde. After washing three times with PBS, the samples were sequentially dehydrated with 50%, 70%, 85%, and 95% ethanol, with one wash for each concentration. The samples were then dehydrated with absolute ethanol three times, each for 15 minutes. After supercritical drying with carbon dioxide, the samples underwent gold sputtering and were observed under a scanning electron microscope (7).

AKP, peptidoglycan, protein, nucleic acid and membrane potential detection in *S. aureus* after Ag^+ treatment

Different concentrations of Ag^+ were diluted in LB liquid medium to predetermined concentrations, and each medium was inoculated with *S. aureus* (OD_{600} = 1.0). After 6 hours, the following indicators were detected. Nucleic acid leakage: Nucleic acid leakage was quantified by measuring absorbance at 260 nm (OD_{260}). AKP

and protein concentration: After centrifugation to collect the supernatant, AKP and protein concentrations were measured. Bacterial lysis for AKP and peptidoglycan content: After centrifugation, the bacteria were lysed to measure AKP and peptidoglycan content. Membrane potential: Membrane potential was evaluated by adding rhodamine (10 μg/mL), followed by incubation in the dark for 30 min. The fluorescence intensity was then measured at 480 nm for excitation and 530 nm for emission.

Invasion and adhesion of *S. aureus* to BEAS-2B cells

S. aureus suspensions were adjusted to an OD_{600} of 0.6. Ag^+ was added to different concentrations (0, 0.25, 0.5, 1, 2, and 4 μM), followed by incubation for 4 hours. Afterward, the bacteria were harvested, resuspended in DMEM, and used to infect BEAS-2B cells at a MOI of 100 (bacteria-to-cell ratio of 100:1) for 3 h.

For the adhesion assay, the cell monolayers were rinsed three times with PBS. Then, 1 mL of 0.2% Triton X-100 was added, and the contents were mixed by pipetting up and down ten times. The lysates were incubated at 37 ℃ for 10 minutes, diluted 1000-fold, and plated on agar plates for colony counting (8).

For the invasion assay, the culture medium was replaced with 1 mL of antibiotic-containing medium and incubated for 1 hour. The cells were washed three times with PBS, and 1 mL of 0.2% Triton X-100 was added. After vigorous pipetting ten times, the lysates were incubated at 37 ℃ for 10 minutes. The samples were then diluted 1000-fold, and colony-forming units were determined on agar plates (9).

Cell toxicity of *S. aureus* on BEAS-2B cells

The concentration of *S. aureus* was adjusted to an OD_{600} of 0.6. Various concentrations of Ag^+ (0, 0.25, 0.5, 1, 2, and 4 μM) were added to the bacterial suspension, which was incubated for 4 hours. The bacteria were then collected, resuspended in DMEM, and used to infect BEAS-2B cells at a bacteria-to-cell ratio of 100:1 (MOI = 100). The infection was allowed to proceed for 12 h. Cytotoxicity was

assessed using the CCK-8 assay.

Effect of Ag^+ on the biofilm formation of *S. aureus*.

Overnight cultures of S. aureus were diluted to 1.0×10^7 CFU. The experiment comprised a bacterial control, a blank control, and seven treatment groups, each containing 200 μL of bacterial suspension. Ag^+ was administered to the treatment groups at final concentrations corresponding to 1/2, 1/4, 1/8, 1/16, 1/32, 1/64, and 1/128 of the IC_{50}, while control groups received an equal volume of ddH_2O. Samples were incubated at 37 ℃ for 48 h.

After incubation, the medium was carefully removed, and wells were gently washed twice with sterile distilled water, followed by air-drying in a biosafety cabinet. Biofilms were stained with 200 μL of 1% crystal violet for 15–20 min, after which excess dye was discarded and the wells were rinsed with 300 μL sterile distilled water. Plates were inverted on absorbent paper to remove residual moisture and allowed to dry at room temperature or 37 ℃.

For quantification, bound crystal violet was solubilized with 200 μL of 33% acetic acid and incubated at 37 ℃ for 30 min. Absorbance was then measured at 590 nm (10).

Effect of Ag^+ on the inflammation response of BEAS-2B cells induced by *S. aureus*

S. aureus suspensions were adjusted to an OD_{600} of 0.6. Ag^+ was added at concentrations of 0, 0.25, 0.5, 1, 2, and 4 μM, and the mixtures were incubated for 4 hours. The treated bacteria were then harvested, resuspended in DMEM, and used to infect BEAS-2B cells at a multiplicity of infection (MOI) of 100 (bacteria-to-cell ratio of 100:1). The infection was allowed to proceed for 24 hours. NO levels in the supernatants were measured using the Griess reagent, following the manufacturer's instructions (Solarbio, China). The concentrations of TNF-α (ml064303), IL-1β (ml058059), and IL-6 (ml058097) in the cell culture supernatants were quantified according to the protocols provided by Shanghai Enzyme-linked Biotechnology Co., Ltd.

Resistance development assay

The resistance frequency of *S. aureus* to antibiotics was evaluated in a sequential generation manner. First, the IC_{50} values of Ag^+ and amoxicillin against *S. aureus* were determined, as described previously. Next, each sub-MIC concentration of antibiotics was re-diluted to 3×10^5 c.f.u./mL and used for the next-generation MIC determination. This procedure was repeated for 14 passages (11).

Bioinformatic analysis

Abundance changes were considered significant based on the criteria of absolute fold change ≥ 1.5 and a P-value (FDR) < 0.05. Subsequently, a volcano plot was generated using the Bioladder website (https://www.bioladder.cn). The proteome function database of *S. aureus* (Taxonomy ID 1279) was downloaded from the UniProt website (https://www.uniprot.org/).

Statistical analysis

Data are expressed as mean ± standard error of the mean (SEM). Statistical analyses were conducted using one-way ANOVA in GraphPad Prism 8.0 (San Diego, CA, USA), with $P < 0.05$ considered indicative of statistical significance.

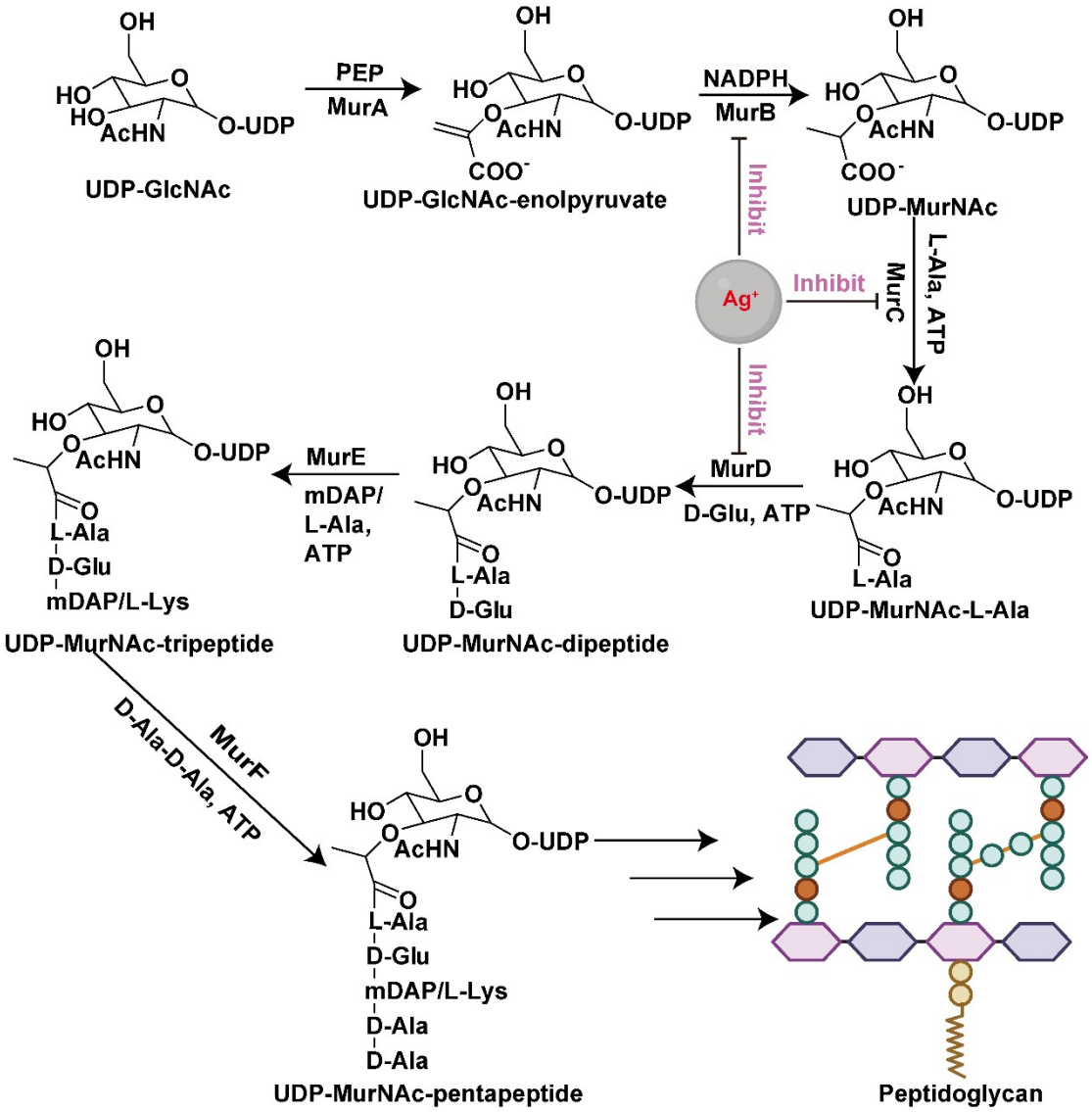

Figure S1. Biosynthesis of peptidoglycan in *S. aureus*. This figure illustrates the biosynthetic pathway of peptidoglycan in *S. aureus*, highlighting the key enzymes involved in its synthesis. The process begins with the formation of UDP-MurNAc-pentapeptide, which serves as the precursor for peptidoglycan. The enzymes MurA to MurF catalyze the sequential steps in the cytoplasm, leading to the generation of the lipid-linked intermediates. These intermediates are subsequently transported across the cytoplasmic membrane, where further modifications and polymerization occur to form the peptidoglycan structure. The final peptidoglycan layer plays a critical role in maintaining the structural integrity of the bacterial cell wall.

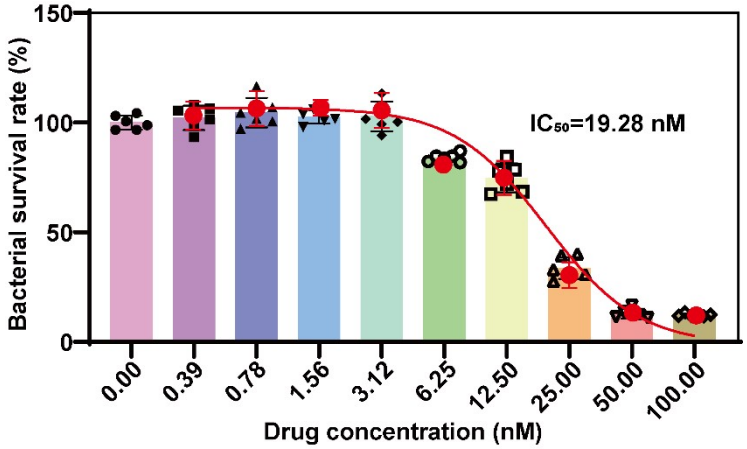

Figure S2. Bacterial survival rate of *S. aureus* following 24 h of treatment with amoxicillin at various concentrations (n = 6).

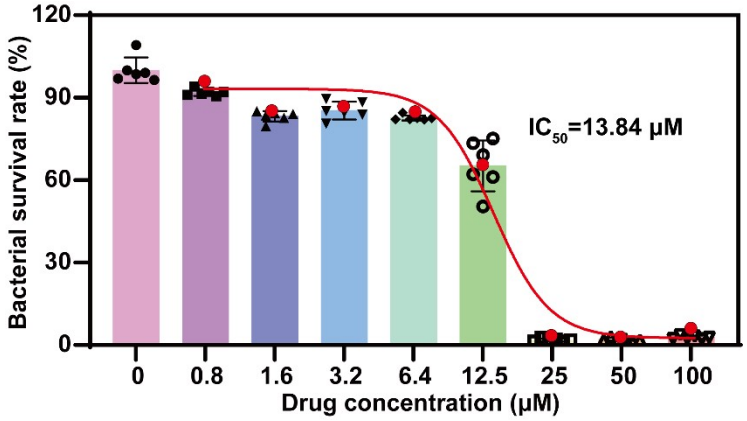

Figure S3. Bacterial survival rate of *Escherichia coli* following 24 h of treatment with Ag^+ at different concentrations (n = 6).

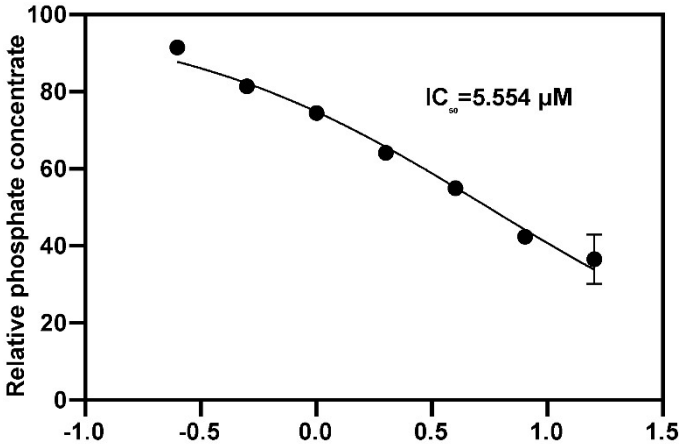

Figure S4. 50% inhibitory concentrations (IC_{50}) of Ag^{+} on the enzymatic activity of WT murC protein.

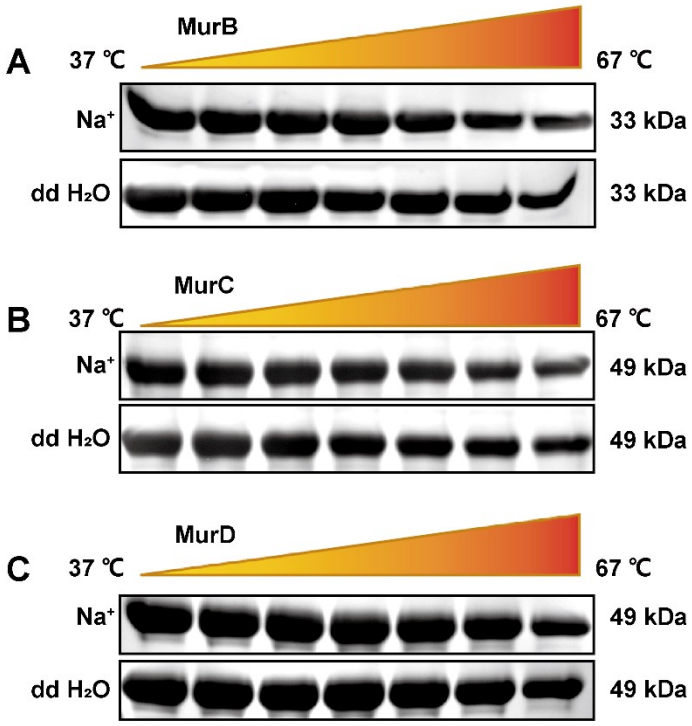

Figure S5. (A) Protein-based thermal shift assays showing the thermal stability of MurB in the absence and presence of Na^+ (1 μM). (B) Protein-based thermal shift assays showing the thermal stability of MurC in the absence and presence of Na^+ (1 μM). (C) Protein-based thermal shift assays showing the thermal stability of MurD in the absence and presence of Na^+ (1 μM).

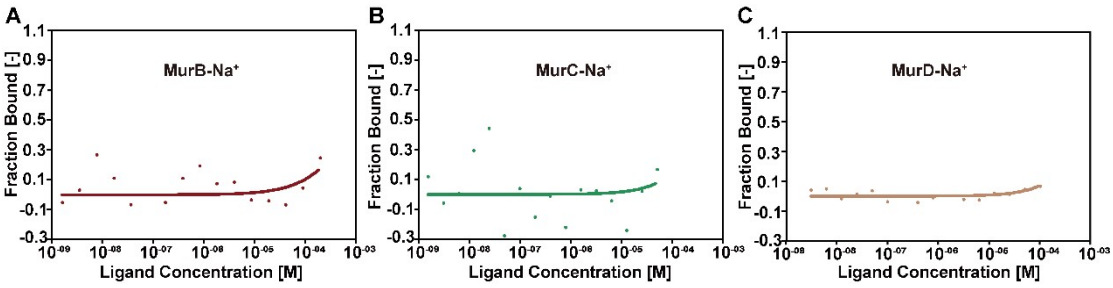

Figure S6. (A) The binding affinity of MurB to Na^+, measured by microscale thermophoresis. (B) The binding affinity of MurC to Na^+, measured by microscale thermophoresis. (C) The binding affinity of MurD to Na^+, measured by microscale thermophoresis.

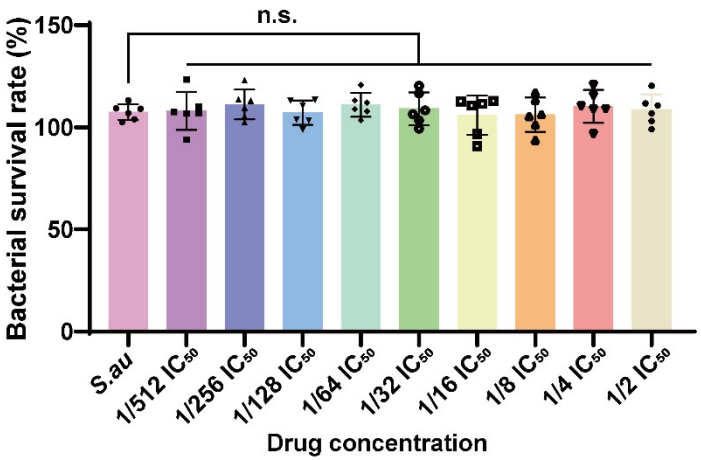

Figure S7. Bacterial survival rate of *S. aureus* following 24 h of treatment with Ag^{+} at concentrations used in the biofilm assays(n=6).

Reference

(1) Lázár, V.; Snitser, O.; Barkan, D.; Kishony, R. Antibiotic combinations reduce Staphylococcus aureus clearance. Nature 2022, 610 (7932), 540-546. DOI: 10.1038/s41586-022-05260-5.
(2) Stoye, A.; Juillard, A.; Tang, A. H.; Legac, J.; Gut, J.; White, K. L.; Charman, S. A.; Rosenthal, P. J.; Grau, G. E. R.; Hunt, N. H.; et al. Falcipain Inhibitors Based on the Natural Product Gallinamide A Are Potent in Vitro and in Vivo Antimalarials. J Med Chem 2019, 62 (11), 5562-5578. DOI: 10.1021/acs.jmedchem.9b00504.
(3) Yuan, Z.; Wang, J.; Qu, Q.; Zhu, Z.; Xu, M.; Zhao, M.; Sun, C.; Peng, H.; Huang, X.; Dong, Y.; et al. Celastrol Combats Methicillin-Resistant Staphylococcus aureus by Targeting Δ(1) -Pyrroline-5-Carboxylate Dehydrogenase. Adv Sci (Weinh) 2023, 10 (25), e2302459. DOI: 10.1002/advs.202302459.
(4) Guo, Y.; Ji, F.; Qiao, J.; Dong, X.; Wu, Y.; Wang, X. Overexpression of the key genes in the biosynthetic pathways of lipid A and peptidoglycan in Escherichia coli. Biotechnol Appl Biochem 2023, 70 (1), 374-386. DOI: 10.1002/bab.2364.
(5) Fiuza, M.; Canova, M. J.; Patin, D.; Letek, M.; Zanella-Cléon, I.; Becchi, M.; Mateos, L. M.; Mengin-Lecreulx, D.; Molle, V.; Gil, J. A. The MurC ligase essential for peptidoglycan biosynthesis is regulated by the serine/threonine protein kinase PknA in Corynebacterium glutamicum. J Biol Chem 2008, 283 (52), 36553-36563. DOI: 10.1074/jbc.M807175200.
(6) Hesse, L.; Bostock, J.; Dementin, S.; Blanot, D.; Mengin-Lecreulx, D.; Chopra, I. Functional and biochemical analysis of Chlamydia trachomatis MurC, an enzyme displaying UDP-N-acetylmuramate:amino acid ligase activity. J Bacteriol 2003, 185 (22), 6507-6512. DOI: 10.1128/jb.185.22.6507-6512.2003.
(7) El Zoeiby, A.; Sanschagrin, F.; Darveau, A.; Brisson, J. R.; Levesque, R. C. Identification of novel inhibitors of Pseudomonas aeruginosa MurC enzyme derived from phage-displayed peptide libraries. J Antimicrob Chemother 2003, 51 (3), 531-543. DOI: 10.1093/jac/dkg010.
(8) Zhang, S.; Qu, X.; Tang, H.; Wang, Y.; Yang, H.; Yuan, W.; Yue, B. Diclofenac Resensitizes Methicillin-Resistant Staphylococcus aureus to β-Lactams and Prevents Implant Infections. Adv Sci (Weinh) 2021, 8 (13), 2100681. DOI: 10.1002/advs.202100681.
(9) Prystopiuk, V.; Feuillie, C.; Herman-Bausier, P.; Viela, F.; Alsteens, D.; Pietrocola, G.; Speziale, P.; Dufrêne, Y. F. Mechanical Forces Guiding Staphylococcus aureus Cellular Invasion. ACS Nano 2018, 12 (4), 3609-3622. DOI: 10.1021/acsnano.8b00716.
(10) Yuan, Z.; Lin, C.; He, Y.; Tao, B.; Chen, M.; Zhang, J.; Liu, P.; Cai, K. Near-Infrared Light-Triggered Nitric-Oxide-Enhanced Photodynamic Therapy and Low-Temperature Photothermal Therapy for Biofilm Elimination. ACS Nano 2020, 14 (3), 3546-3562. DOI: 10.1021/acsnano.9b09871.
(11) Guo, F.; Xiao, F.; Song, H.; Li, X.; Xiao, Y.; Qin, Y.; Lei, X. An Optimized Marinopyrrole A Derivative Targets 6-Phosphoglucosamine Synthetase to Inhibit Methicillin-Resistant Staphylococcus aureus. ACS Cent Sci 2024, 10 (11), 2090-2098. DOI: 10.1021/acscentsci.4c01167.